ELSEVIER

abm

Original Article

A new concept of auxiliary fuel injection through tuyeres in blast furnaces developed by numerical simulations

CrossMark

Bruno Orlando de Almeida Santos[a], Breno Totti Maia[a,], Fabricio Silveira Garajau[a], Marcelo de Souza Lima Guerra[a], Paulo Santos Assis[b], José Eduardo Mautone Barros[c]*

[a] *Lumar Metals Research, Santana do Paraíso, MG, Brazil*
[b] *Universidade Federal de Ouro Preto (UFOP), Escola de Minas, Ouro Preto, MG, Brazil*
[c] *Universidade Federal de Minas Gerais (UFMG), Av. Antônio Carlos, 6627, Pampulha, MG, Brazil*

ARTICLE INFO

ABSTRACT

The Injection of powdered materials in blast furnaces is a great option for reducing costs, increasing productivity and satisfy the environmental norms. Thus, this paper presents a study on the use of a flame stabilization system with rotation, designed to promote greater coal injection in the combustion zone, reducing losses and increasing the efficiency of the equipment. A physical model was used to evaluate scattering of pulverized fuel and is compared with numerical results in the same scale. In the second step, a combustion model was added to the numerical simulation, using dimensions of a real blast furnace. Fields like temperature, velocity and behavior of chemical reactions were analyzed. The results showed that double lances promote better particle injection when compared with simple lance for reduced material injection. The new injection system proposed, with swirl numbers of 0.12 and 0.24, promoted a better injection of both reduced material and temperature in the raceway zone. The swirl 0.24 showed superior performance when compared to other injection systems.

1. Introduction

The injection of pulverized materials through the tuyeres of blast furnaces is one of the great achievements in steel industry. Currently, pulverized coal has become a very important supplementary fuel, which contributes to generate heat, reducing operating costs, stabilize operation and reduce carbon dioxide emission.

However, if the rate of pulverized coal injection (PCI) is increased, the percentage of unburned coal increases. The material which is not burned crosses the combustion zone boundary and enters into the furnace, reducing permeability and affecting blast furnace stability.

In this scenario, there will be a maximum amount of coal that can be burned at the combustion zone. The relationship between the coal rate and combustion rate, was determined by Assis [1,2].

Increased coal rate injection above the maximum limit causes the combustion rate to be effected and the blast furnace stability will be compromised. The technological development for pulverized coal injection (PCI) has been extensively recognized throughout the world [3].

In pursuit of higher injection rates of fluid material with good blast furnace permeability, several mechanisms are being continuously tested, such as mixture of coals as well as coal injection combined with new materials such as tires, rice husks and sugar cane. This also includes projects to inject gas and fuel by double co-axial pipe lance.

The fluid is treated continuously to analyze the macroscopic properties such as velocity, pressure, density and temperature, and its derivatives in space and time. Properties like the microscopic structure and molecular motions are ignored. Variables in the governing equations converted to gas phase include mass, momentum, energy, chemical particles and turbulence. As to the particle phase, they include momentum and energy (Table 1) [3,4].
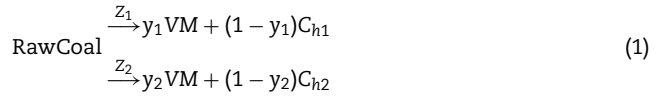
Where: "ρ" density; "U" velocity; "S_m" Mass added in continuous phase; "t" stress strength; "g" gravity; "F" external forces; "h_{tot}" total enthalpy; "S_E" external forces; "p" pressure; "t" time; "k" kinetic energy; "Y_i" chemical particles; "J_i" diffusion flow of particles; "μ" dynamic viscosity; "μ_t" turbulent viscosity; "ε" kinetic energy dissipation; "C_μ, $C_{\varepsilon 1}$, $C_{\varepsilon 2}$, σ_k, σ_ε" turbulence models constants [5]; "P_{kb}" buoyancy forces; "$P_{\varepsilon b}$" turbulence production due to viscous forces; "F_D" drag forces; "F_B" buoyancy forces due to gravity; "F_R" rotation forces in domain; "F_{Um}" force due to mass added; "F_P" forces due to pressure; "m_C" mass; "Cp" specific heat; "Q_C" convection heat transfer; "Q_M" heat transfer due to mass; "Q_R" radiation heat transfer.

As for carbon particles, they must be reactive and products can be found in other phases or gas phase. The burning is calculated from injected rate particle's equations combined with turbulent calculation of dissipation for volatiles combustion in gas phase [6,7].

The combustion of coal can be divided into four stages: heating, raw coal devolatilization, gaseous combustion and volatile materials oxidation as well as gasification of carbonized material by residual gas phase turbulence. The devolatilization and carbon oxidation process can occur in milliseconds. This time is much smaller than a typical residence time of particles during transport in the combustion zone. Large variations in time scale equations can result in large numbers, causing problems on the results accuracy [8].

The devolatilization can be modeled by one or more reaction steps using an Arrhenius reaction with generic multiphase capacity, where process is usually represented by one or two steps of reaction. Shen et al. [7,9] used a model with two competing reactions and different constants of reactions (Z_1, Z_2) and actual volatiles yield (y_1 and y_2):

$$\text{RawCoal} \begin{array}{c} \xrightarrow{Z_1} y_1 VM + (1 - y_1)C_{h1} \\ \xrightarrow{Z_2} y_2 VM + (1 - y_2)C_{h2} \end{array} \qquad (1)$$

where "VM" mass fraction of volatile material and "C_k" residual coal burned. Often volatile yield of materials from each type of coal is known only after immediate analysis in the laboratory, where heating rate is low and volatiles that escape may undergo secondary reactions including breakage and carbon deposition on solid surfaces.

$$\frac{d}{dt} d_p = C_s d_{0,p} \frac{\dot{m}_{ref}}{m_{ref,0}} \qquad (2)$$

where "d_p" diameter of particle current, "C_s" increase coefficient, "$d_{0,p}$" particle diameter in the early devolatilization, "$\dot{m}_{ref}$" change mass rate of reference and "$m_{ref,0}$" reference mass early devolatilization.

Two models are proposed for carbonized material oxidation, the Field model and the Gibbs model. Shen et al. [9,10] compares these two models. In the Field model just external diffusion of reactive gases to particle surface is considered. Thus, the burned material was overestimated, and the authors recommended a model that considers more detailed mechanisms. The authors used Gibbs model, where internal diffusion in particles by gaseous species are considered. Rate diffusion and chemical reaction equation are considered in rate global carbon reaction, like in Eq. (3):

$$\frac{dm_c}{dt} = (k_d^{-1} + k_c^{-1})^{-1} X_g 4\pi R_p^2 \frac{P}{P_A} \qquad (3)$$

where "k_d" diffusion rates for oxygen; "k_c" diffusion rates for carbon; "X_g" molar fraction of oxygen into furnace.

The reactions are being controlled by the lower diffusion rates "k_d" and "k_c". The Eddy Dissipation Model (EDM) is based on rapid chemical reaction in relation to transport process flow

Table 1 – Governing Equations for the gas and particle phase.			
Gas phase	Mass		$\frac{\partial \rho}{\partial t} + \nabla \cdot \left(\rho \vec{U} \right) = S_m$
	Momentum		$\frac{\partial}{\partial t}(\rho U) + \nabla \cdot \left(\rho \vec{U}\vec{U} \right) = -\nabla p + \nabla \cdot \left(\bar{\bar{\tau}} \right) + \rho \vec{g} + \vec{F}$
	Energy		$\frac{\partial(\rho h_{tot})}{\partial t} - \frac{\partial p}{\partial t} + \nabla \cdot (\rho U h_{tot}) - \nabla \cdot (k\nabla T) + \nabla \cdot (U.\tau) + U \cdot S_M + S_E$
	Gas species i		$\frac{\partial}{\partial t}(\rho Y_i) + \nabla \cdot \left(\rho \vec{U} Y_i \right) = -\nabla \cdot \vec{J}_i + R_i + S_i$
	Turbulent kinetic energy		$\frac{\partial(\rho k)}{\partial t} + \frac{\partial}{\partial x_j}(\rho U_j k) = \frac{\partial}{\partial x_j}\left[\left(\mu + \frac{\mu_t}{\sigma_k} \right) \frac{\partial k}{\partial x_j} \right] + P_k - \rho\varepsilon + P_{kb}$
	Turbulent dissipation rate		$\frac{\partial(\rho\varepsilon)}{\partial t} + \frac{\partial}{\partial x_j}(\rho U_j \varepsilon) = \frac{\partial}{\partial x_j}\left[\left(\mu + \frac{\mu_t}{\sigma_\varepsilon} \right) \frac{\partial \varepsilon}{\partial x_j} \right] + \frac{\varepsilon}{k}(C_{\varepsilon 1}P_k - C_{\varepsilon 2}\rho\varepsilon + C_{\varepsilon 1}P_{\varepsilon b})$
Particle Phase	Momentum		$m_p \frac{dv_p}{dt} = F_D + F_B + F_R + F_{VM} + F_P$
	Energy		$\sum(m_C C_P)\frac{dT}{dt} = Q_C + Q_M + Q_R$

by assuming that, when reactants are mixed, they form products instantly. The model chosen by Shen et al. [11] assumes that the reaction rate is directly related to time required for mixing reagents at molecular levels.

For turbulent flow, the mixing time is based on recirculation's properties, and its rate, defined by turbulent kinetic energy "k" and turbulent dissipation "ε" [12,13] (Eq. (4)):

$$\text{Rate} \propto \frac{\varepsilon}{k} \tag{4}$$

The model of dissipation by borders is constantly used in industrial problems. The reaction rate is faster as compared with the rate of reagents mixing. The boundary of a given reaction is determined by reactants, Eq. (5), products, Eq. (6), whichever comes first:

$$R_k = A \frac{\varepsilon}{k} \min \left(\frac{[I_m]}{v'_{KI}} \right) \tag{5}$$

$$R_k = AB \frac{\varepsilon}{k} \left(\frac{\sum_p (I_m) W_{I_m}}{\sum_p v''_{KI} W_{I_m}} \right) \tag{6}$$

where "I_m" is the molar concentration of component "I".

The rotational flows are mechanisms characterized by spiral flow application, which can be achieved when transmitting tangential velocities in perfectly axial flows. The twist degree applied has a significant impact on flow results. The flow characterization is done by measuring the velocity profile. Twist degree is measured by a dimensionless number, "S", which represents axial flow torque, "G_θ" divided by product of moment axial flow, "G_z", and equivalent radius, "R_t", as:

$$S = \frac{G_\theta}{G_z R_t} \tag{7}$$

$$G_\theta = \int_0^R \left(\rho v_z v_\theta + \overline{\rho U'_z U'_\theta} \right) . r^2 dr \tag{8}$$

$$G_z = \int_0^R \left(\rho U'^2_z + \rho \overline{U^2_z} + (p - p_\infty) \right) r dr \tag{9}$$

Fluid rotation has been widely used in the industry. The principal applications are heat and mass exchangers, turbines, burners, particle separators. It is also applied to control the pneumatic conveying in line pressure drop.

2. Results and discussion

To study pulverized fuel behavior in tuyeres, considering the conditions of spreading and spraying, as well as chemical reactions and combustion efficiency, the following steps are adopted. Step 1 – Physical test in reduced scale (1:4,8) shown in Fig. 1, using cold-compressor with maximum flow approximately 189Nm3/h available at LaSiP (Laboratory for Process Simulation), School of Engineering, Federal University of Minas Gerais. Step 2 – Changing tuyere types, with CFD simulation validating the results of physical cold simulation. Step 3 – CFD simulation for combustion into tuyeres with fine coal
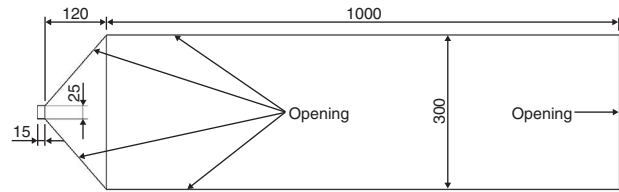

Fig. 1 – Computational geometry, in millimeters, of the cold physical model.

injected into blast furnace that produce 700 tons of Hot Metal (HM)/day in scale 1:1.

The tests were carried out using cold air at ambient temperature representing air through tuyeres. The fuel was represented by cornstarch sprayed with grain sizes ranging between 30 and 100 microns. In this step combustion is not considered. The set used in cold tests had small-scaled dimensions of 1:4.8 for blast furnace of 700 tons per day of hot metal, and 150 kg per ton of pulverized coal injection rate (Table 2).

To avoid interference of walls over the flow field, the experiment was conducted in an open environment, where two white stripes, 300 mm distant from each other, were used to delineate catchment images area. To blow air through tuyeres, a 22.5 kW compressor was used to produce 7.87×10^5 Pa pressure and a maximum flow of approximately 189 N m^3/h. Flow meters and pressure were used to control and measure air conditions before tuyeres entrance, to ensure specified achievement of experiment conditions. To assess particles dispersion degree, a high definition camera (full HD) capable of capturing up to 60 frames per second was used.

To meet the proposed objectives, experiments were performed varying the tuyere configurations while all other parameters were held constant. The goal is to check particle injection behavior into the raceway.

The computational geometry that represents physical cold model chosen is based on a scale 1:4.8 tuyere furnace, with a diameter of 25 mm and 3 mm for gas injection and pulverized material. Four configurations of pulverized coal injection were compared, using single lance, dual lance, lance with twist factor S = 0.12 and lance with twist factor S = 0.24.

To work with data close to the actual data from blast furnace studied in this work, the dimensions shown in Fig. 2 were used. The region bounded by domain is restricted to data obtained from scaling the combustion zone, considering 5 m diameter from furnace. At this stage, domain-scale 1:1 was chosen to represent in greater detail the equipment in real operation with various injection techniques tested.

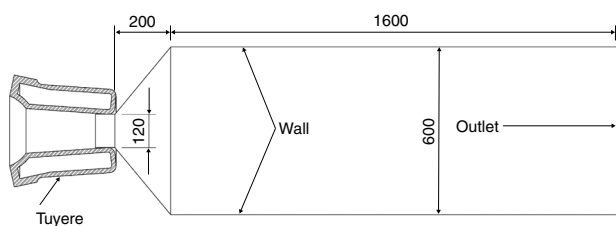| Table 2 – Cold physical simulation conditions.	
	Reduced scale [1:4.8]
Air injection velocity	100 m/s
Coal mass flow	0.014 kg/sec
Conveying gas velocity	15 m/s
Air temperature	25 °C

Fig. 2 – Computational geometry, in millimeters, of the coal combustion zone.

Table 3 – Coal combustion data.

Description	Unit	Present Work	Shen et al.
Blast velocity	m/s	140	137
Blast temperature	K	1273	1473
Particles	kg/tHM	150	80–190
C	[%]	74.05	89.1
H	[%]	5.31	4.70
N	[%]	1.60	1.70
S	[%]	0.35	0.37
O	[%]	11.99	4.10

To represent real boundary conditions of blast furnace in this study, input parameters were adjusted as operational data (Table 3).

In the tuyeres region, although the mesh varies due to geometry of each configuration, the total number of nodes was around 450,000, reducing variations in accuracy due to the mesh. More detailed mesh was received in regions near the tuyeres to allow better capture with precision initial spread, soon after pulverized fuel injection, and air injected influence into trajectory prediction of particles throughout the domain. Fig. 3 represents different mesh configurations of powdered material injection with statistics mesh.

Due to tuyeres complexity geometry, the loop control factors were monitored to ensure only hexahedron elements.

When comparing settings of simple lance and double lance with new settings $S = 0.12$ and $S = 0.24$, one can observe that turbulence effect generated by incoming air provides greater scattering and increases S factor. This is because centrifugal speed acting on the particle causes increased spreading rate and a greater effect is observed near tuyeres exit.

Fig. 4 shows the relationship between injection type and spreadability obtained in the combustion region. The results presented in Fig. 4a and b show that for single lance, the spreadability angle obtained is 12° and for double lance, the spreadability is almost 30% higher. The greater spread of fuel provided by dual lance allows a wider range for the lances in the combustion zone, when compared with simple lance. Thus, it allows increased combustion efficiency, as already stated by Maki et al. [8]. The increased combustion efficiency allows higher rates of injection, since lower likelihood of bird's nest formation due to not burned coal. Following these concepts, the swirl lances improved the rate of spreading around 58% for $S = 0.12$ and 100% for $S = 0.24$, when compared with single lance.
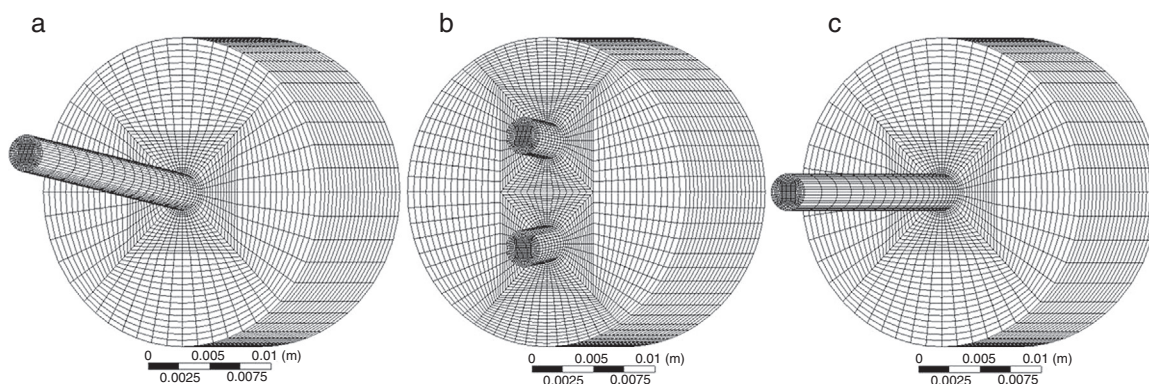

Fig. 3 – Different mesh configuration: (a) lance single, (b) dual lance and (c) twist factors $S = 0.12$ and $S = 0.24$.
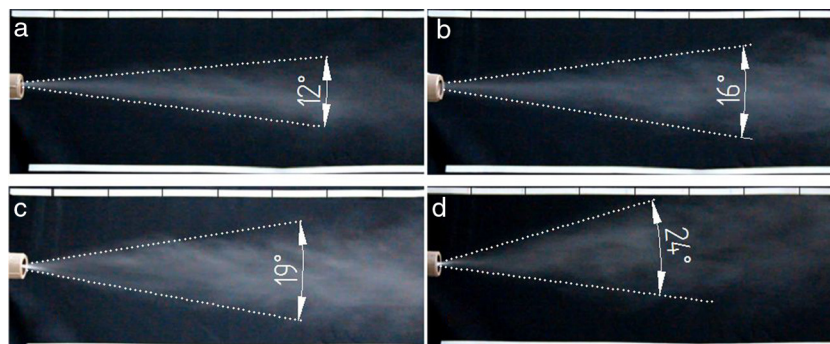

Fig. 4 – Effect of spreading injected material into tuyeres (a) lance single, (b) dual lance (c) twist factor $S = 0.12$ and (d) twist factor $S = 0.24$.
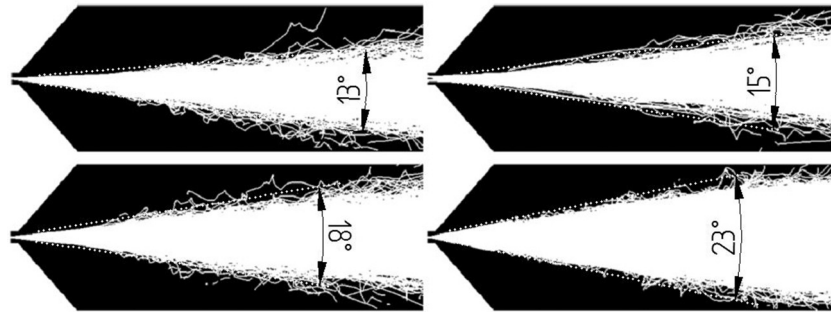
Fig. 5 – Spreading predicted by the numerical model.

Table 4 – Surface spread area of pulverized coal.					
	Physical simulation		Numerical simulation		Difference
	Angle (°)	Area (m^2)	Angle	Area (m^2)	%
Lance simple	12	0.071	13	0.074	4.22
Double lance	16	0.091	15	0.090	1.10
$S = 0.12$	19	0.106	18	0.105	0.94
$S = 0.24$	24	0.132	23	0.131	0.75

Whereas, length of combustion zone, which has a strong relationship with input speed by heated air, was not significantly altered by different settings evaluated tuyeres. The second step is to evaluate particulate phase injected behavior into computational domain. To assess behavior and accuracy of models chosen, simulation results were compared with results obtained in physical tests (Fig. 5).

To quantify the physical results and to compare with numerical results, the surface combustion area, bounded by spreading presented in Table 4, were calculated.

Thus, there is a strong influence of continuous field in particles because of size. It can be seen in Fig. 6 that finer particles spread mix with jet center. Since, particles are larger and heavier, they are crowded in a big chunk in the runoff, dispersing farther from tuyeres exit. Particle size distribution in the domain exists in a simple lance, is shown in Fig. 6(a). It has the highest concentration of large particles in the jet center and other systems providing greater spread. The system shown in Fig. 6(d), which has a twist factor, $S = 0.24$, in addition, provides the highest spreadability and the highest dispersion of larger particles.

When comparing different types of results for injection in this work, it is possible to see different behavior of flame in the combustion zone. Fig. 7 shows the temperature profile for different injection methods. When comparing sets of twist $S = 0.12$ and $S = 0.24$ with others, one observes an increase in heat input, especially the latter, which provides a superior firing power over others.

Increasing the twist factor, burning of pulverized coal occurs near the tuyeres exit. The largest spreadability promoted by $S = 0.24$ system allows larger particles to spread closer the tuyeres exit, providing a greater mix of gas and particles in the combustion zone. The radiation of heat by metal loading and heated air promotes rapid combustion, reducing the residence time, releasing volatile and burning almost instantly. This condition is evident in Fig. 8, when comparing maximum temperature in four different types of injection.

An increase in efficiency of burning coal is also observed (Fig. 9), using $S = 0.24$, where the average temperature of combustion zone rises rapidly near tuyeres exit due to increased spreadability and mixing of pulverized fuel. Subsequently, decreasing temperature at end of combustion zone was
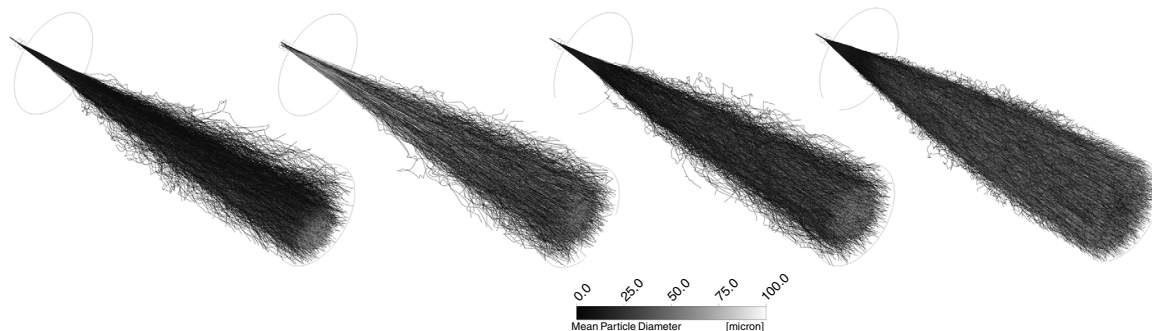

Fig. 6 – Size distribution of particles in the injection systems (a) lance single, (b) dual lance (c) twist factor $S = 0.12$ and (d) twist factor $S = 0.24$.
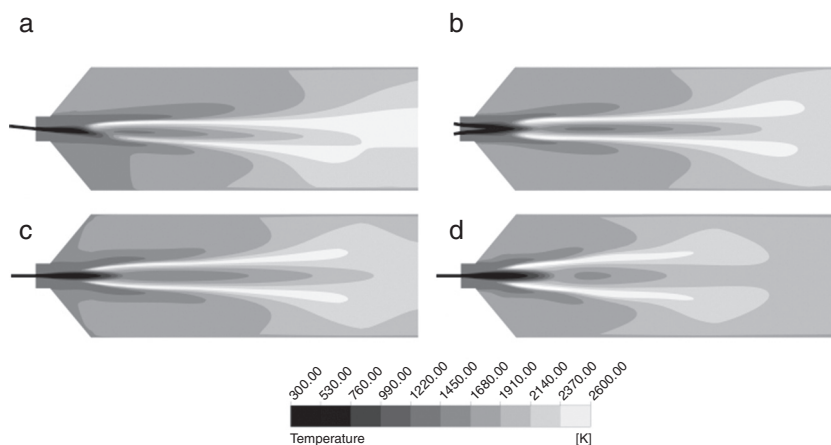
Fig. 7 – Temperature profiles for injections types (a) lance single, (b) dual lance, (c) twist factor S = 0.12 and (d) twist factor S = 0.24.
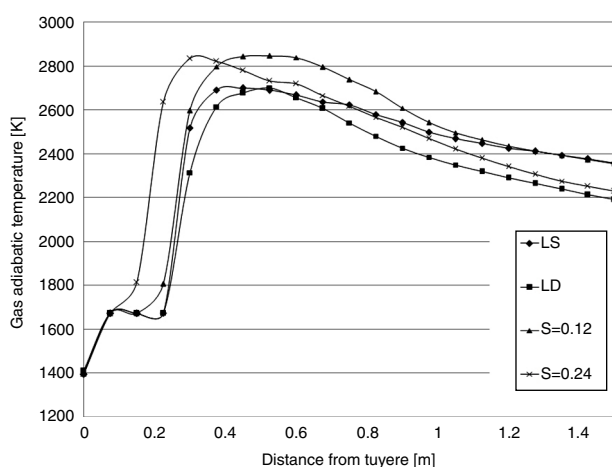

Fig. 8 – Comparison of gas temperature in combustion zone for different injection methods studied.

Fig. 9 – Average temperature of the combustion zone for different injection methods studied.

associated with the reduction of combustion rate, due to carbon for reaction. This behavior is observed only in this configuration, and other injection systems (LS, DL and S = 0.12) have a lower temperature near tuyeres and evolving as coal is burned.

The curves related to the behavior obtained in Fig. 9 presents a possibility of increasing the injection rate using S = 0.24. It is expected to burn fuel without deposition of coal, due to the highest efficiency. When Shen et al. model (Fig. 10) and swirl model S = 0.24 are compared, it can be observed that the mean gas temperature in the combustion zone is very similar, even with lower inlet temperature, 1000 °C against 1200 °C used by Shen et al. [11].

For injection system S = 0.12, one can see in Fig. 11c that, despite the formation of a dense core of small particles, there is also a greater spread of particles that are in the periphery of the nucleus and were influenced by rotation's vectors of injected air. This phenomenon is more evident when a stronger twist factor S = 0.24 is used (Fig. 11d). It is observed in this configuration that there are no longer core particles, which are distributed with greater uniformity in the combustion zone, which promotes a more efficient burning.
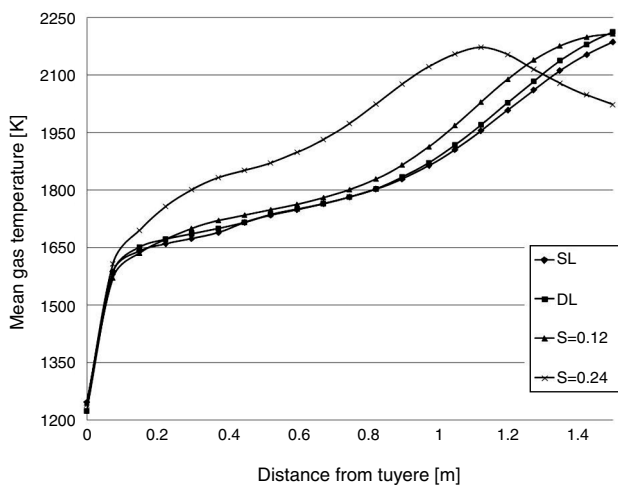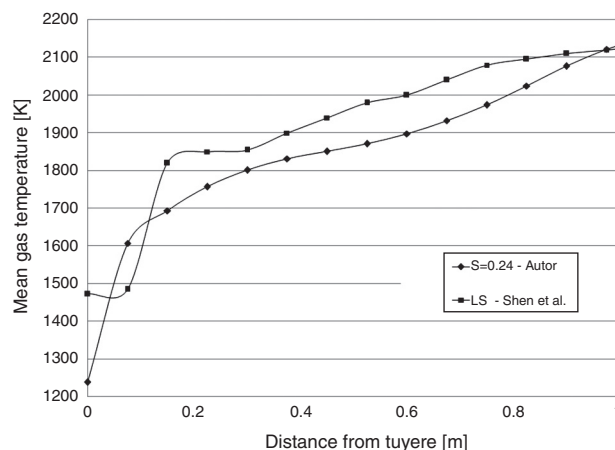

Fig. 10 – Comparison between the simple lance tested by Shen et al. and the injection system with twist factor S = 0.24 of this work.
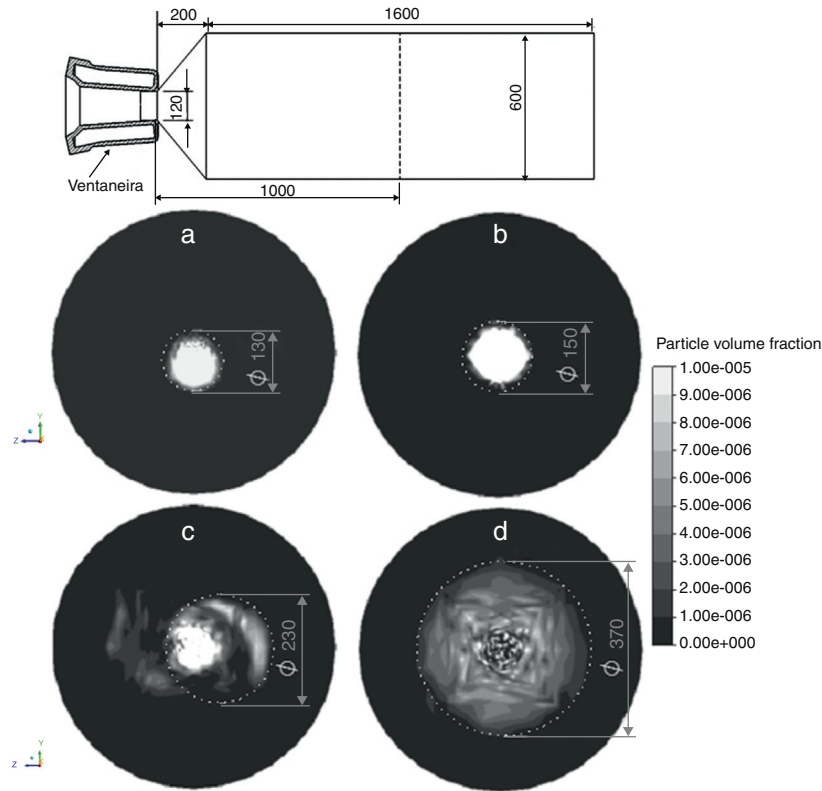
Fig. 11 – Volumetric fraction of fuel (a) lance single, (b) dual lance, (c) twist factor $S = 0.12$ and (d) twist factor $S = 0.24$. Cross section at 1 m from exit tuyere. Measurements in millimeters.

The methods of fuel injection sprayed through single and double releases, commonly used in industry, have a slow-spreadability behavior, since the particle moves away from tuyeres exit. Already in the injection systems with a twist, this scattering grows stronger as it moves away from the tuyere. Fig. 12 illustrates the effect provided by twist method compared with LS and DL methods.

The particle traveling through the combustion zone suffers continuous phase effects, represented by incoming air. Thus, when a particle is carried by a continuous phase with twist effect, this is launched by flow that spreads more and more as it travels through the area.

In the case of injection systems LS and LD, particles of smaller diameter suffer, first, the effects of flow, and then, those of the larger diameter. Therefore a greater distance is required for the particles to center spread. On systems with twist factors $S = 0.12$ and $S = 0.24$, the effect is felt also by the heavier particles. The trend is toward a spreadability increase near tuyeres exit with increasing twist factors.
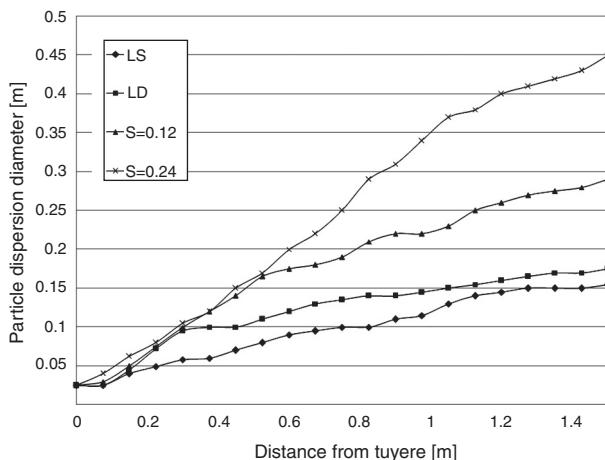
3.   Conclusions

The effect of different methods of injecting pulverized fuel in blast furnace tuyeres, where physical tests and numerical tools were used to validate theoretical assumptions raised in the literature review, was discussed in this paper.

Initial results indicated that particles behavior captured during physical simulation performed very similar to those obtained with numerical simulation. The spreadability of pulverized coal showed significant differences with variation in the injection systems. Comparing results up to 1 m away from the tuyeres exit, dual lances, $S = 0.12$ and $S = 0.24$, showed average increases of approximately 26%, 75% and 111%, respectively.

Comparing results of average temperature in combustion zone for fuel injection systems with LD and LS, it is possible to observe similar values, with average growth of about 1% higher for LD system. However, when compared to

Fig. 12 – Evolution of the coal spreading into the combustion zone.

conventional systems, LS and LD, and systems proposed by the author for, S = 0.12 and 0.24, it is possible to observe large increases in the average temperature of the combustion zone. Average increasing was found to be 2% and 7%, respectively.

However, when comparing the injection system used with LS, the injection system S = 0.24 in this work had a higher initial spreadability of pulverized fuel and rapid rise in temperature of combustion zone, even with air temperature below 200 °C in comparison with other authors. The results showed that the evolution of the average temperature in the combustion zone for fuel injection system with S = 0.24 and blowing temperature of 1000 °C are comparable to a simple lance system with a temperature of 1200 °C breath. It is believed that higher rates of injection can be used in blast furnaces operating with charcoal and plants that have Glendons as air heaters.

In all parameters, the injection system S = 0.24 was more efficient, and the factor S = 0.12 showed similar results to system LD. LS, single lance, had the poorest results.

The comparison between results in this work with results obtained by other authors in literature, showed that the injection method S = 0.24 is more efficient in terms of spreadability of particles, mixing and burning. The combustion model must still be validated in laboratory and industrial practice. Several important variables were not evaluated in this study and should be investigated in greater depth before experimental tests.

Conflicts of interest

The authors declare no conflicts of interest.

Acknowledgments

REFERENCES

[1] Assis PS, Dr. Dissertation at RWTH-Aachen Einblasen von Holkohle in den Holzkohlehochofen; 1991. p. 124.

[2] Assis PS. Injeção de materiais pulverizados em altos-fornos. Belo Horizonte: Associação Brasileira de Metalurgia e Materiais; 2009.

[3] Seshadri V, Tavares RP, Silva CA, Silva IA. Fenômenos de transporte: fundamentos e aplicações nas Engenharias Metalúrgica e de Materiais". BELO HORIZONTE: ABM; 2010, 01.

[4] Hauke G. An introduction to fluid mechanics and transport phenomena. Zaragoza: Springer; 2008.

[5] Wilcox David C. Turbulence modelling for CFD. 1st ed. California: DCW Industries, Inc.; 1993.

[6] CFX. CFX 12.1 – "Solver Theory Guide", USA; 2010.

[7] Shen Y, Guo P, Zulli P. Model study of the effects of coal properties and blast furnace conditions on pulverized coal combustion. ISIJ Int 2009;49:819–26.

[8] Maki A, Sakai A, Takagaki N, Mori K, Ariyama T, Sato M, et al. High rate coal injection of 218 kg/t at Fukuyama No. 4 blast furnace. ISIJ Int 1996;36:650–7.

[9] Shen YS, Guo BY, Zulli P, Maldonado D, Yu ABA. Three-dimensional cfd model for coal blends combustion: model formulation and validation". In: Fifth International Conference on CFD in the Process Industries. 2006.

[10] Shen YS, Guo BY, Yu AB, Austin PR, Zulli P. Three-dimensional of in-furnace coal/coke combustion in a blast furnace. Fuel 2011;90:728–38.

[11] Shen Y, Guo B, Maldonado D, Austin P, Zulli P. Three-dimensional modeling of coal combustion in blast furnace. ISIJ Int 2008;48:777–86.

[12] Sharma SP, Mohan C. Fuels and combustion. New Delhi: Tata McGraw-Hill Publishing Company Limited; 1984.

[13] Guo B, Zulli P, Rogers H, Mathieson JG, Yu AB. Three-dimensional simulation of flow and combustion for pulverized coal injection. ISIJ Int 2005;45:1272–81.